Supporting Information: Influence of Gas Packing and Orientation on FTIR activity for CO chemisorption to the Cu Paddlewheel

Table S1. Summary of the existence of Cu^{+}/Cu^{2+} peaks in Cu-TDPAT and Cu-BTC. The color coding represents the control variables.

Sample	Preparation	Pretreatment	2120 cm^{-1} (Cu^{+})	2170 cm^{-1} (Cu^{2+})
Cu-TDPAT				
T_1	No grinding	543 K, 1 min	150 K: N	150 K: N
T_2	Grinding	Not applied	100 K: N	100 K: N
T_3	Grinding	393 K, 10 hr	150 K: N	150 K: N
T_4	Grinding	543 K, 1 min	150 K: N	150 K: N
T_5	No grinding	Not applied	100 K: N	100 K: N
	No grinding	543 K, 1 min	100 K: N	100 K: N
T_6	No grinding	373 K, 60 min	100 K: N	100 K: N
	No grinding	423 K, 30 min	100 K: N	100 K: N
	No grinding	573 K, 1 min	100 K: N	100 K: N
Cu-BTC				
B(SA)_1	No grinding	Not applied	150 K: Y	150 K: N
B(SA)_2	No grinding	543 K, 1 min	150 K: Y	150 K: Y
			200 K: Y	200 K: Weak
			300 K: Y	300 K: N
			400 K: Weak	400 K: N
B(SA)_3	No grinding	633 K, 15 min	150 K: Weak	150 K: N
			200 K: N	200 K: N
			300 K: N	300 K: N
B(RU)	No grinding	543 K, 1 min	150 K: Y	150 K: Y
			200 K: Y	200 K: N
			300 K: Y, blue shift	300 K: N

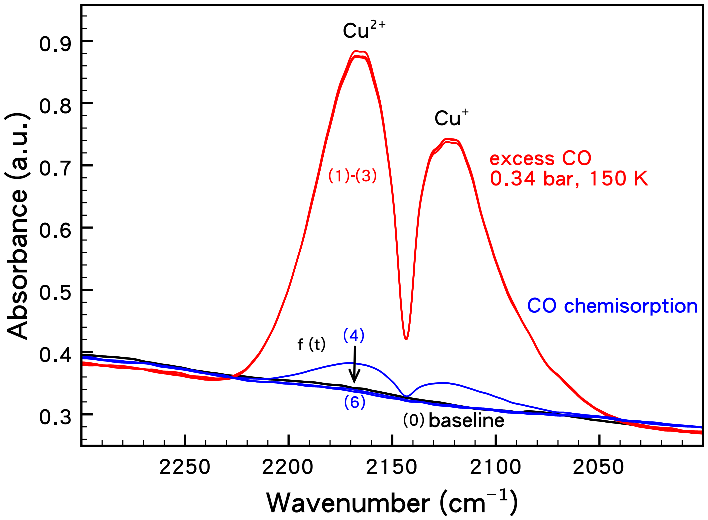

Figure S1. (A) FTIR spectra of **T**_1 (See nomenclature in Table S1) at 150 K in excess CO exposure (1-3) and in Ar purging to remove gas phase CO for CO chemisorption (4-6). The number represents the sequence of each spectrum, where (0) was collected in Ar purging before the sample was exposed to CO. No evidence for CO chemisorption was observed for any pretreatment temperature, adsorption temperature, or sample preparation method. This data is repeated in Figure 7.

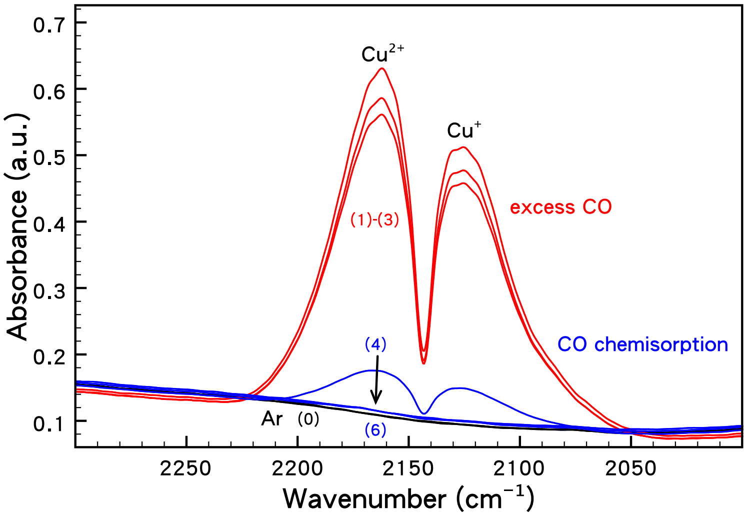

Figure S1. (B) T_2 (Conditions noted in Table S1). Labels as described in (A).

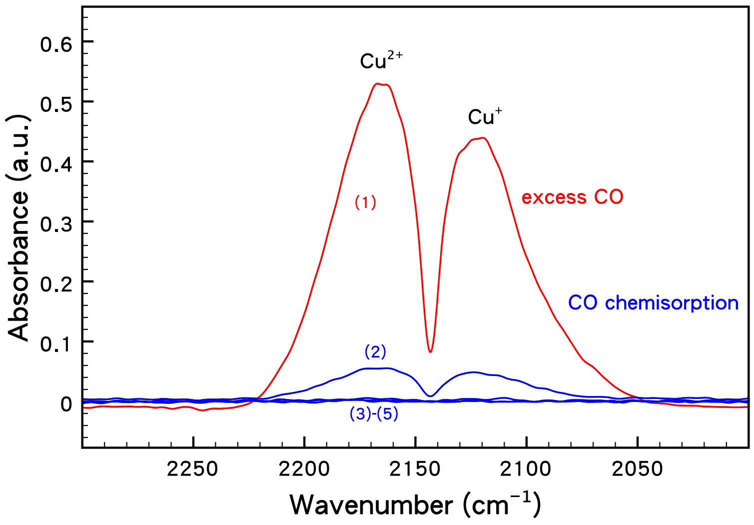

Figure S1. (C) T_3 (See Table S1). Labels as described in (A).

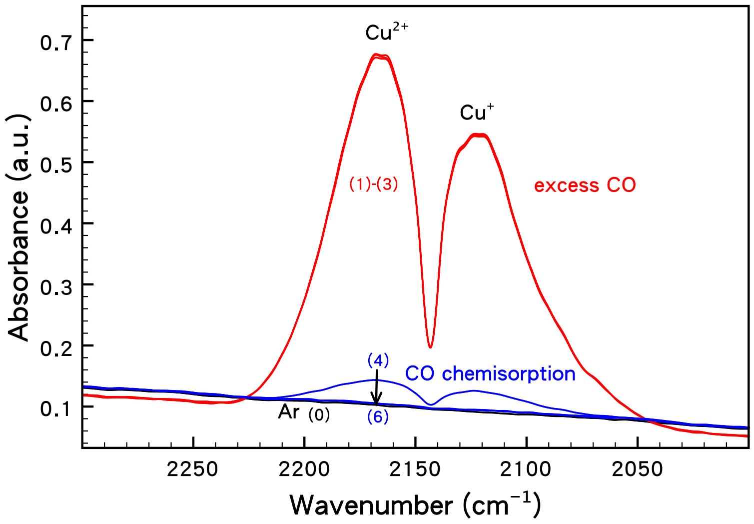

Figure S1. (D) T_4 (See Table S1). Labels as described in (A).

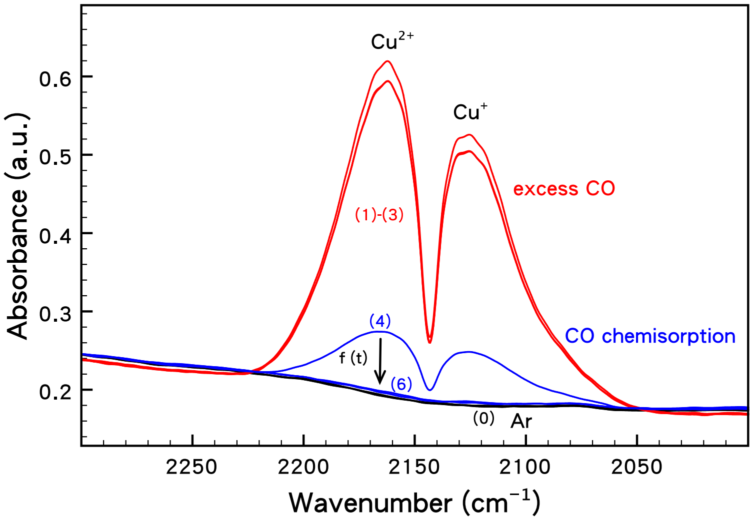

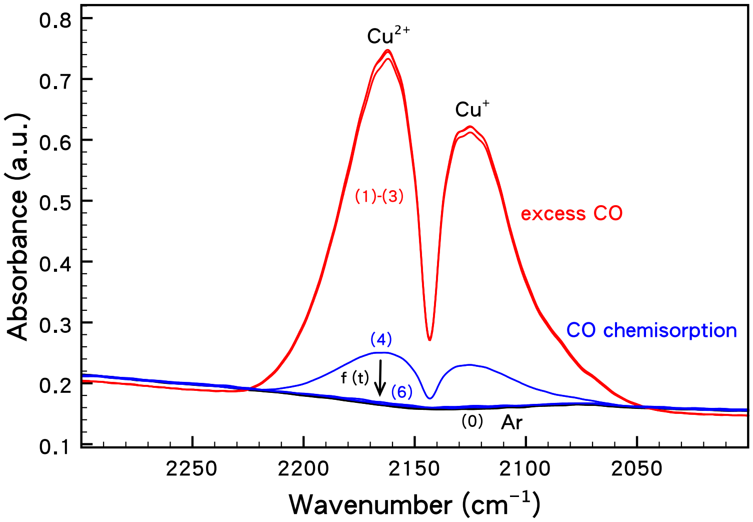

Figure S1. (E) T_5 (See Table S1), without (above) and with (below) pretreatment. Labels as described in (A).

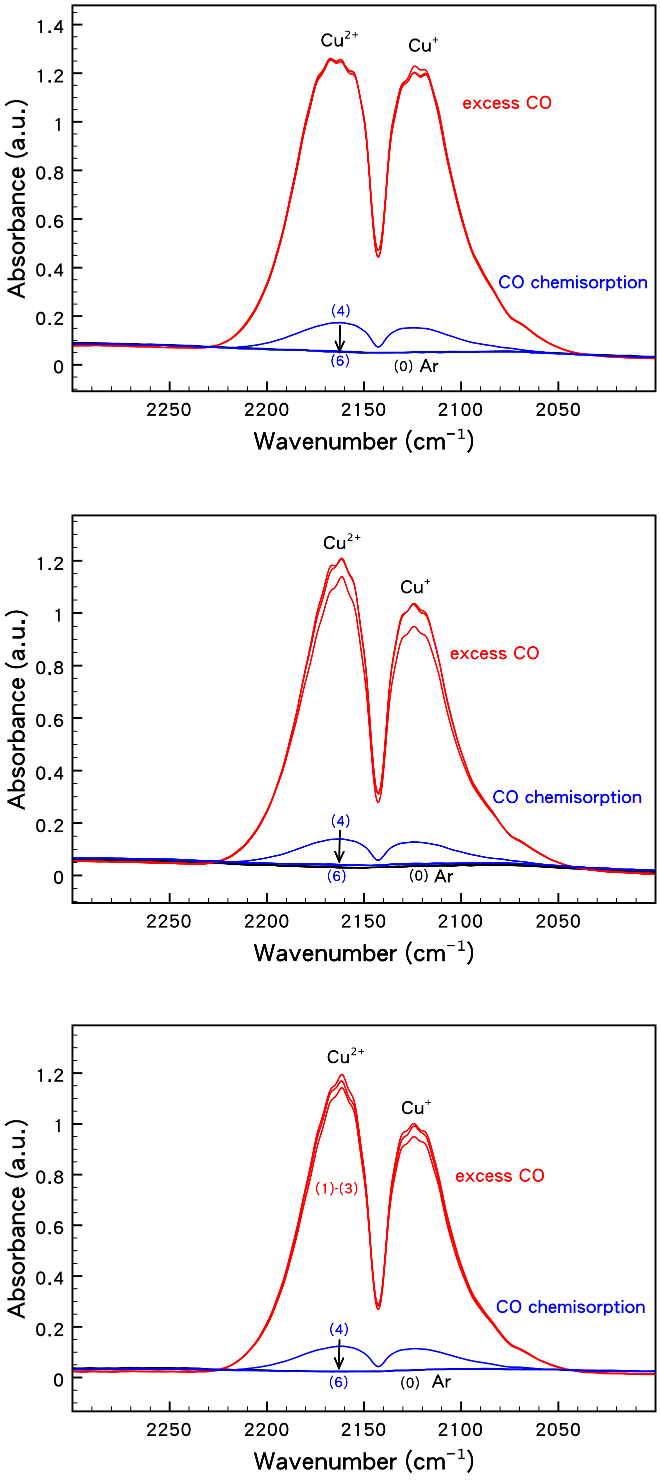

Figure S1. (F) T_6 (See Table S1), preceded by pretreatments at 373 K (top panel), 423 K (middle panel), and 573 K (bottom panel). Labels as described in (A).

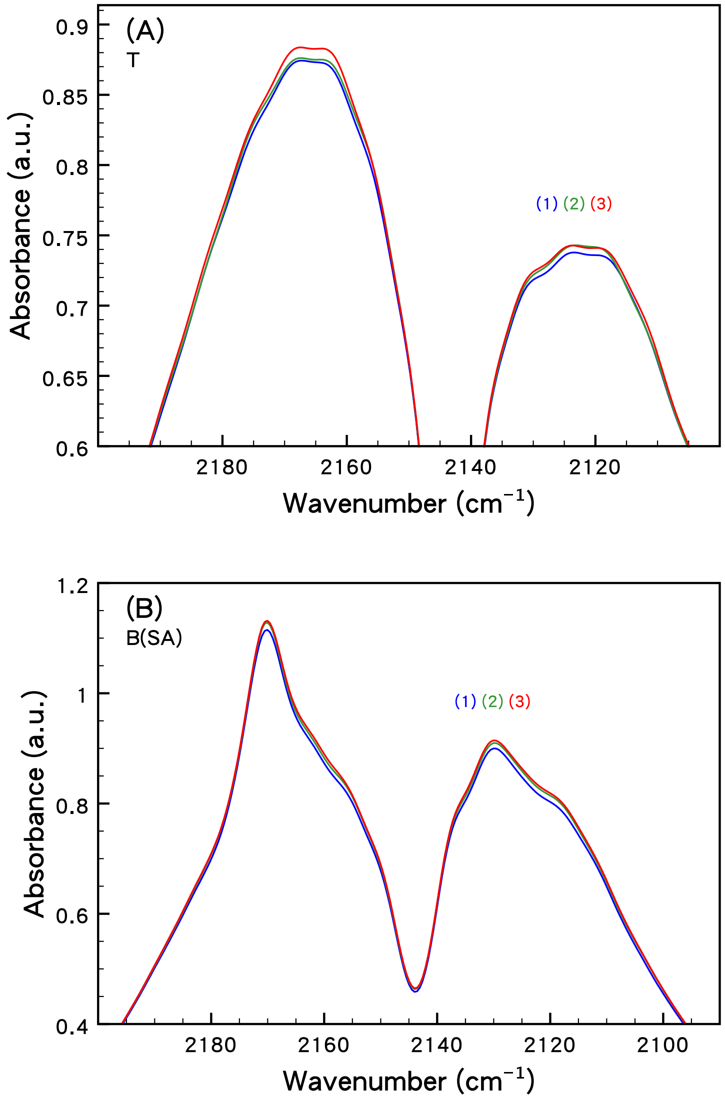

Figure S2: The CO gas phase spectra of (A) **T** and (B) **B**(SA) collected in sequence (spectrum 1 to 3, collected in 10 minutes), after 0.34 bar of CO was reached. It can be found that the peak reaches the steady state with the maximum intensity. Absorbance shown only above >0.4 to highlight the differences between spectra.

To obtain the sub peak positions, we use Gaussian-Lorentzian mixed function (fitting parameters: position, intensity, FWHM, and Gaussian-Lorentzian ratio) with Shirley background fitting. The fitting parameters are tested with initial guessed values in the program.

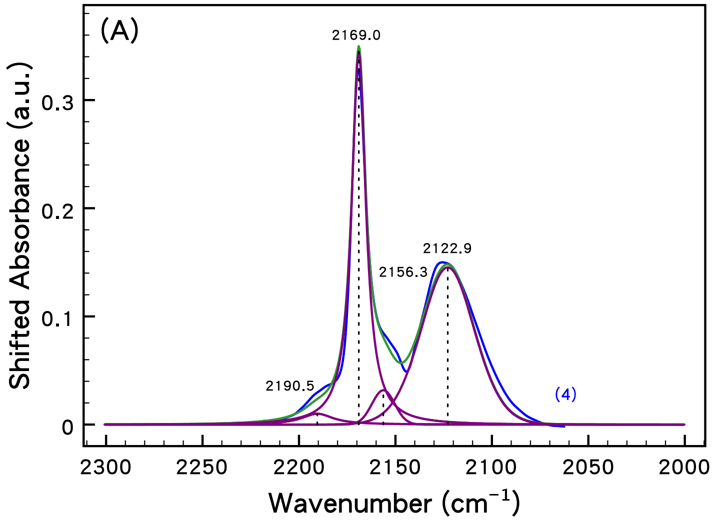

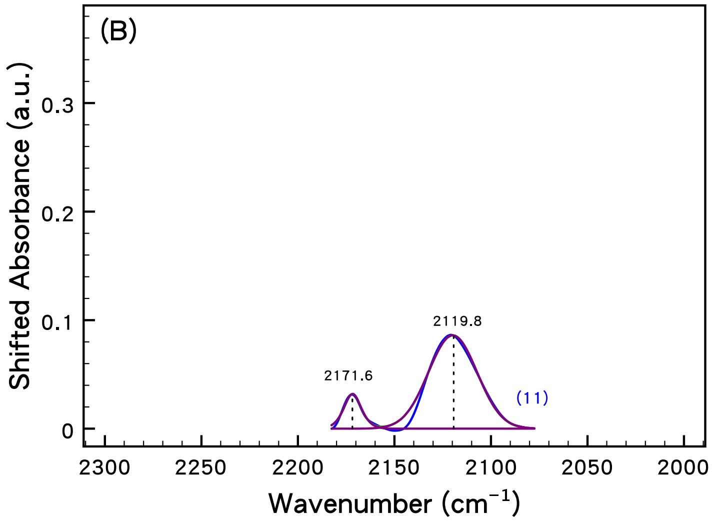

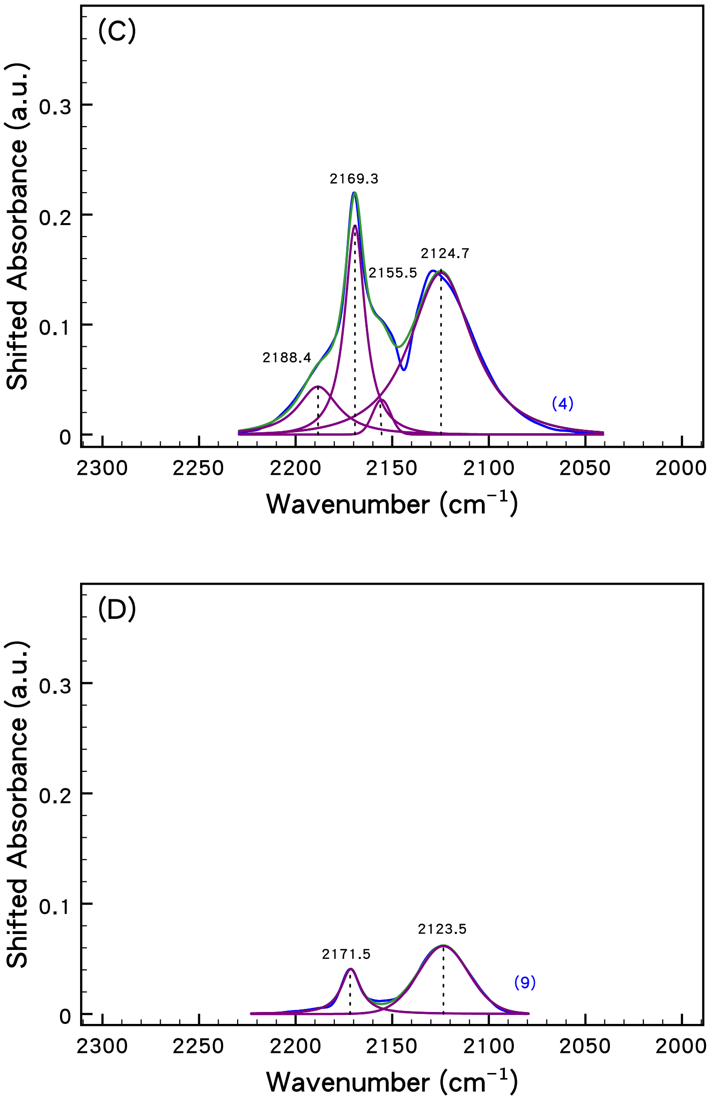

Figure S3. The curve fitting of FTIR spectra of Basolite (**B**(SA)) at 150 K (A: spectrum (4), B: spectrum (11)) and aged Cu-BTC (**B**(RU)-1) at 150 K (C: spectrum (4), D: spectrum (9)) from Figure 5 (Blue: experimental data, purple: fitted individual peak, green: fitted spectrum).

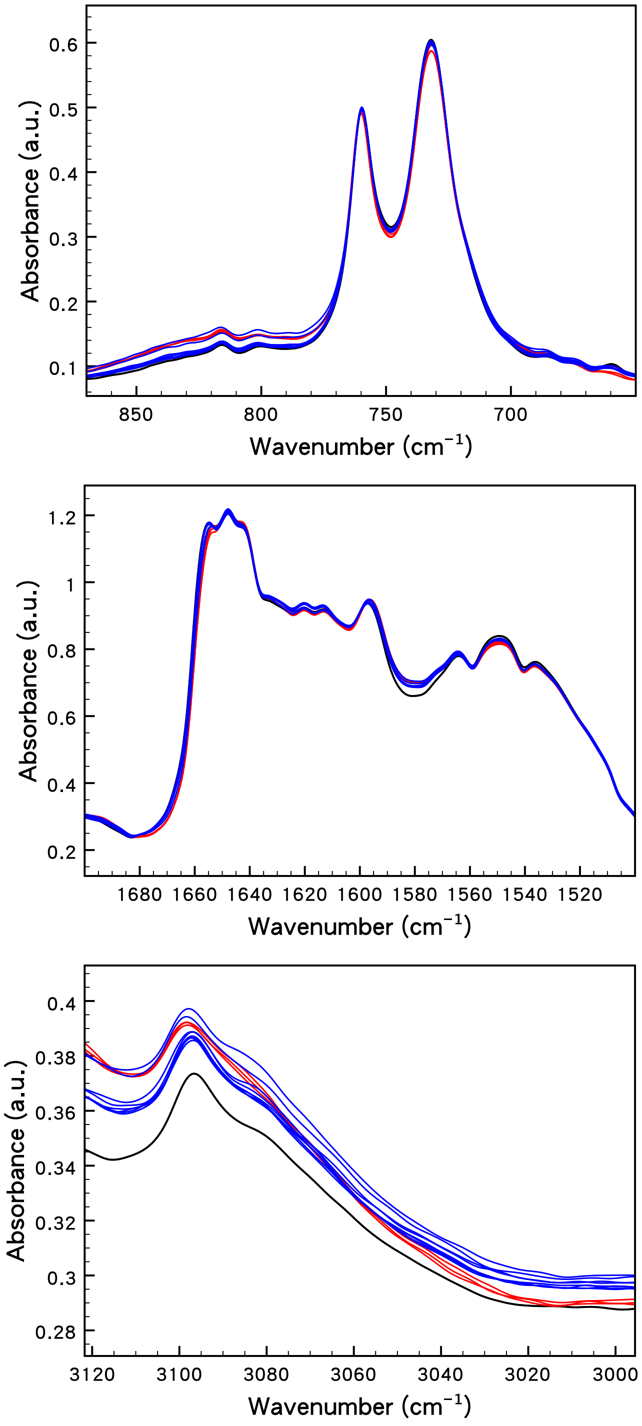

Figure S4: The FTIR spectra of **B**(SA) of Figure 5A at different wavenumber regions at 150 K throughout the test, including initial baseline of the MOF (black), 0.34 bar CO exposure (red), and 0.34 Ar purging (blue). No changes are observed in the aromatic C-H stretch (3000-3100 cm^{-1}), C-H bending (675-870 cm^{-1}), C=C (1500-1600 cm^{-1}), and C=O (1700 cm^{-1}).[1-3]

Redhead Analysis: In order to estimate CO desorption temperature from MOF Cu-BTC, we adopt the Arrhenius equation, where r is the desorption rate, E_a is the activation energy, and v_n is a rate constant; allowing for a generic n^{th} order reaction in terms of coverage θ:

$$r(t) = -\frac{d\theta}{dt} = v_n \theta^n e^{-E_a/RT} \tag{S1}$$

A linear heating rate relates temperature to time as follows:

$$T(t) = T_o + \beta t$$

$$\Rightarrow dt = \frac{1}{\beta} dT \tag{S2}$$

Thus, we can rewrite Eq. S1 as function of temperature T:

$$r(T) = -\frac{\beta d\theta}{dT} = v_n \theta^n e^{-E_a/RT}$$

$$\Rightarrow \frac{d\theta}{dT} = -\frac{1}{\beta} v_n \theta^n e^{-E_a/RT} \tag{S3}$$

Defining T_p as the temperature at which the desorption rate, r,is a maximum, the second derivative of coverage with respect to T will be zero at T_p:

$$\frac{d^2\theta}{dT^2} = -\frac{1}{\beta} v_n (n) \theta^{n-1} \frac{d\theta}{dT} e^{-E_a/RT} - \frac{1}{\beta} v_n \theta^n e^{-E_a/RT} \left(\frac{E_a}{RT^2} \right) = 0 \tag{S4}$$

Insert Eq. S3 to Eq. S5, and assuming a first order desorption process ($n = 1$):

$$\frac{d^2\theta}{dT^2} = -\frac{1}{\beta} v_n (n) \theta^{n-1} \frac{d\theta}{dT} e^{-E_a/RT} + \frac{d\theta}{dT} \left(\frac{E_a}{RT^2} \right) = 0$$

$$\Rightarrow E_a = RT_p \left[\ln \frac{v_n T_p (n) \theta^{n-1}}{\beta} - \ln \left(\frac{E_a}{RT_p} \right) \right]$$

$$\Rightarrow E_a = RT_p\left[\ln\frac{v_1 T_p}{\beta} - \ln\left(\frac{E_{act}}{RT_p}\right)\right] = RT_p\left[\ln\frac{10^{13} T_p}{\beta} - 3.64\right] \tag{S5}$$

where we assume $v_1 \sim 10^{13}$ sec^{-14} and $\ln\left(\frac{E_a}{RT_p}\right) = 3.64$

With Eq. S5, we can estimate the activation energy based on the temperature with highest adsorbate desorption rate *r*, which can be determined from TPD experiments. We use Gaussian-Lorentzian mixed function (fitting parameters: position, intensity, FWHM, and Gaussian-Lorentzian ratio) with non-linear background fitting ($y = Bx^A + C$) to determine TPD profile dr_1/dT peak positions in temperature, shown in Figure S5. The activation energies from the desorption temperature are shown in Table S2.

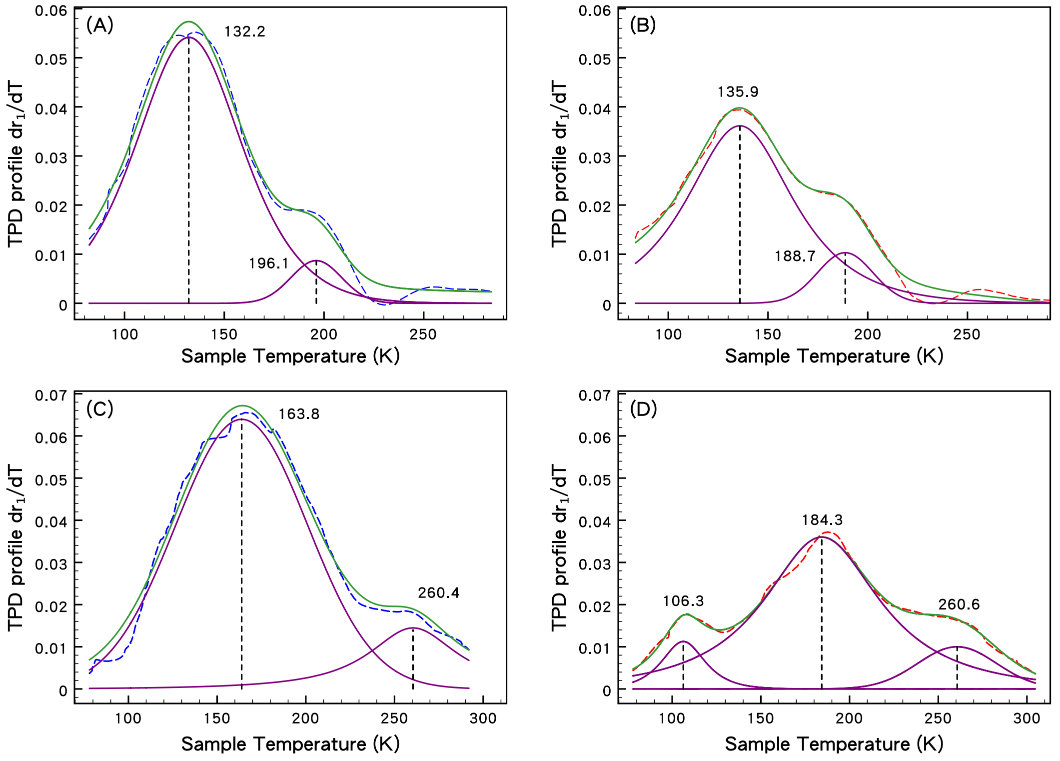

Figure S5. The curve fitting of TPD profile of CO in vacuum (A, B) and in 0.34 bar CO environment (C, D) (Blue: **T**, Red: **B**(SA), purple: fitted individual peak, green: fitted curve).

In addition, we estimate the activation energy based on the temperatures from TD-FTIR experiments with Eq. S7, shown in Table S2.

Table S2: Activation energy and desorption temperature with maximum desorption rate of CO-Cu in **T** and **B**(SA).

Pressure (bar)	MOF	Temperature (K)	Activation Energy (eV)	Activation Energy (kJ/mol)
10^{-5} (vacuum)	**T**	132.2	0.40	38.1
		196.1	0.59	57.2
	B(SA)	135.9	0.41	39.2
		188.7	0.57	54.9
0.34 (CO)	**T**	163.8	0.49	47.5
		260.4	0.79	76.5
	B(SA)	106.3	0.32	30.5
		184.3	0.56	53.6
		260.6	0.79	76.6
0.34 (Ar) (TD-FTIR)	**B**(SA)	~200	0.60	58.3
		~400	1.23	119

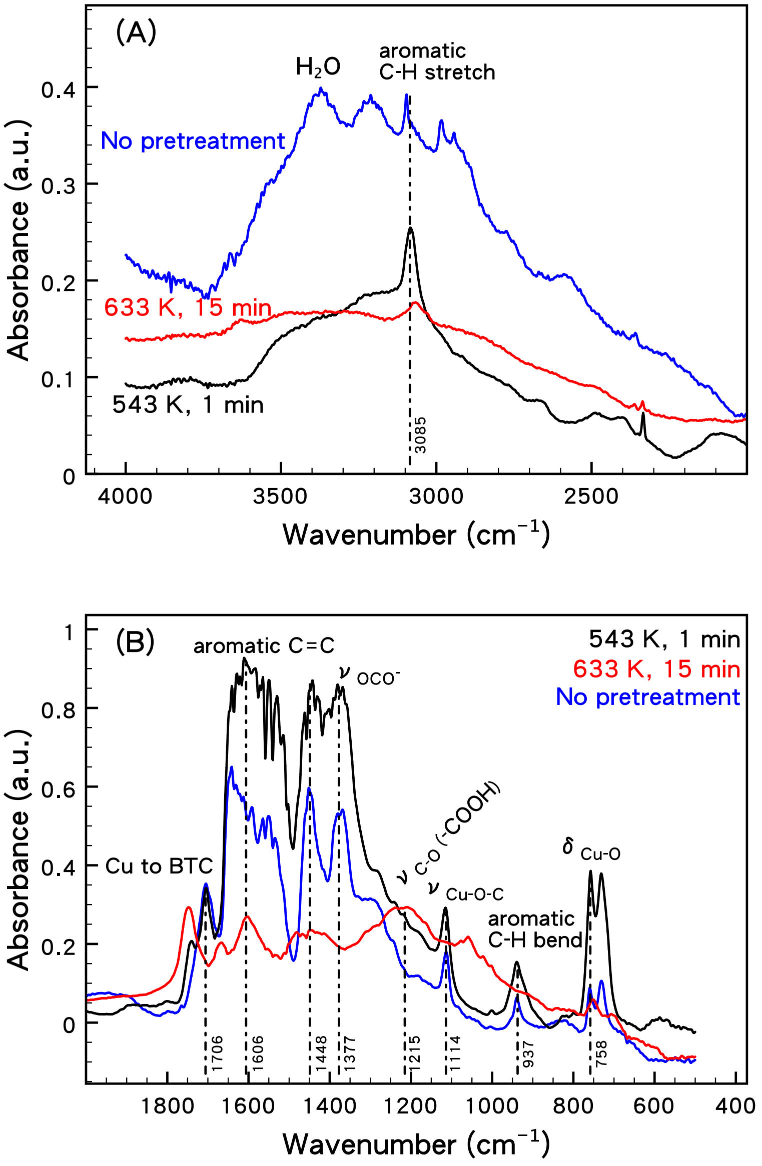

Figure S6. FTIR spectra (higher (A) and lower (B) wavenumber regions) of Basolite (**B**(SA)) under different pretreatment conditions (no pretreatment, 543 K 1 min, and 633 K 15 min) in the baseline (0) spectra, i.e. in flowing Ar before the sample was exposed to CO. A broad O-H stretch at ~3400 cm^{-1} shows clear evidence of water when pretreatment is omitted (blue). After the 633 K pretreatment (red), the Cu-O bending mode (at 758 cm^{-1}) is broadened relative to the other pretreatments, while other Cu-O modes at 1114 cm^{-1} and 1706 cm^{-1} disappear; perhaps most notably, the carboxylic acid (1215 cm^{-1}) mode grows while the peak of carboxylate mode (at 1377 cm^{-1}) disappears.

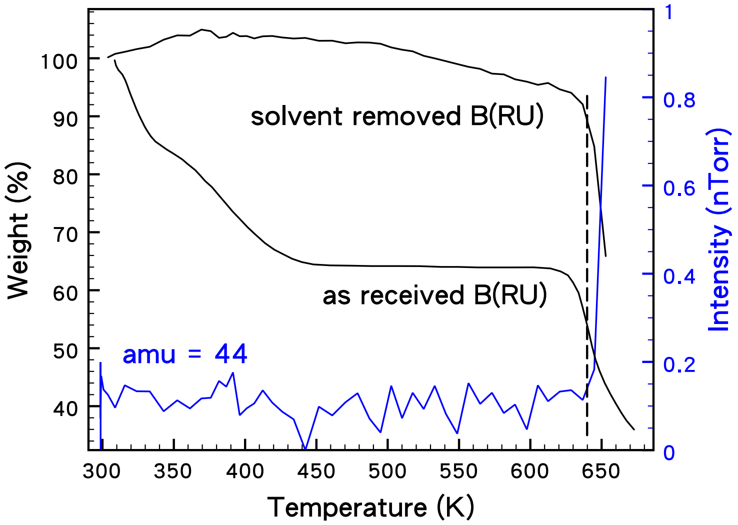

Figure S7. TGA of **B**(RU) under N_2 flow at 25 sccm. The as-received **B**(RU) contains coordinated water, and thus it shows weight loss starting at 300 K. The **B**(RU) that has had solvent removed via a prior pretreatment (423 K 10 hr) retains its weight until over 600 K. The degradation observed at ~640 K for both materials corresponds to evolution of CO_2 (amu=44) with an attached mass spectrometer.

The pore-size distribution (PSD) of **B** estimated via the Horvath-Kawazoe (H-K) method suggests the pores of **B** are <12 Å and 14 – 17 Å (Figure S8). The calculated H-K PSD of **T** is quite broad, with pore sizes ranging from 10 – 20 Å.

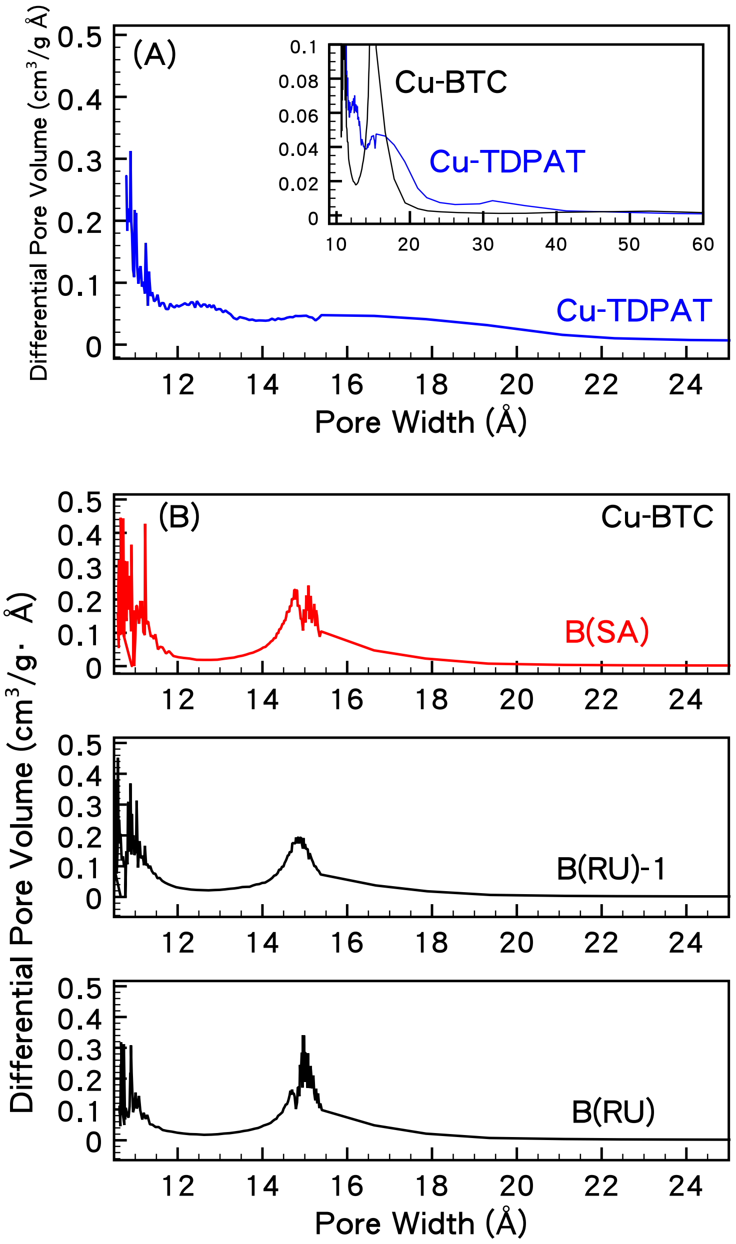

Figure S8. The pore size distribution (PSD) of Cu-TDPAT (A) and Cu-BTC series (B), calculated from the H-K model. The two distinct steps observed in the N_2 isotherm of **B** suggest two size pores. The lack of distinct features in the N_2 isotherm of **T** suggests no distinct adsorption sites.

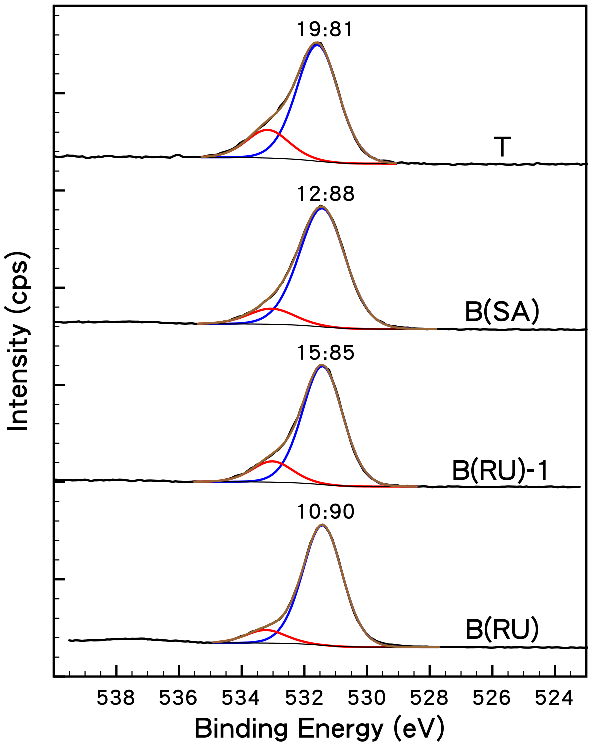

Figure S9. XPS spectra of O 1s spectra for Cu-BTC **B**(RU), **B**(RU)-1, **B**(SA), and Cu-TDPAT (**T**).

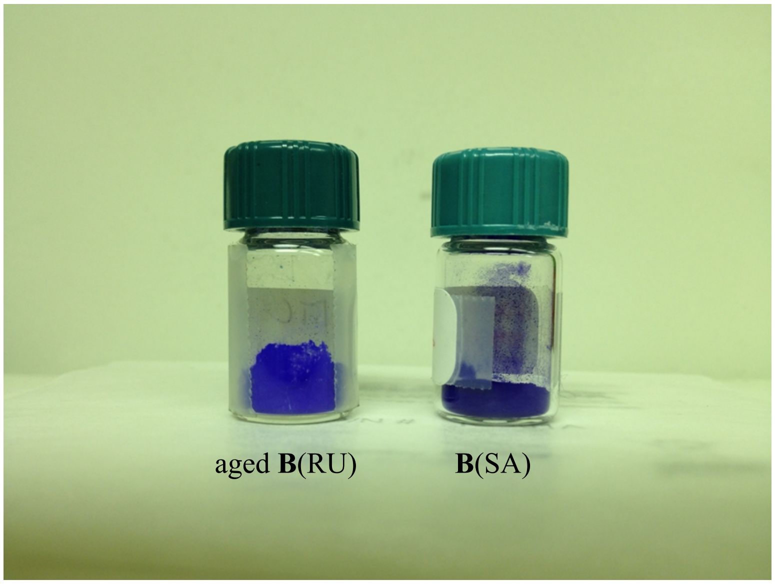

Figure S10: The photo of Cu-BTC **B**(RU) and **B**(SA). Both samples were pretreated to remove residual solvent and stored in a glove box with inert gas Ar.

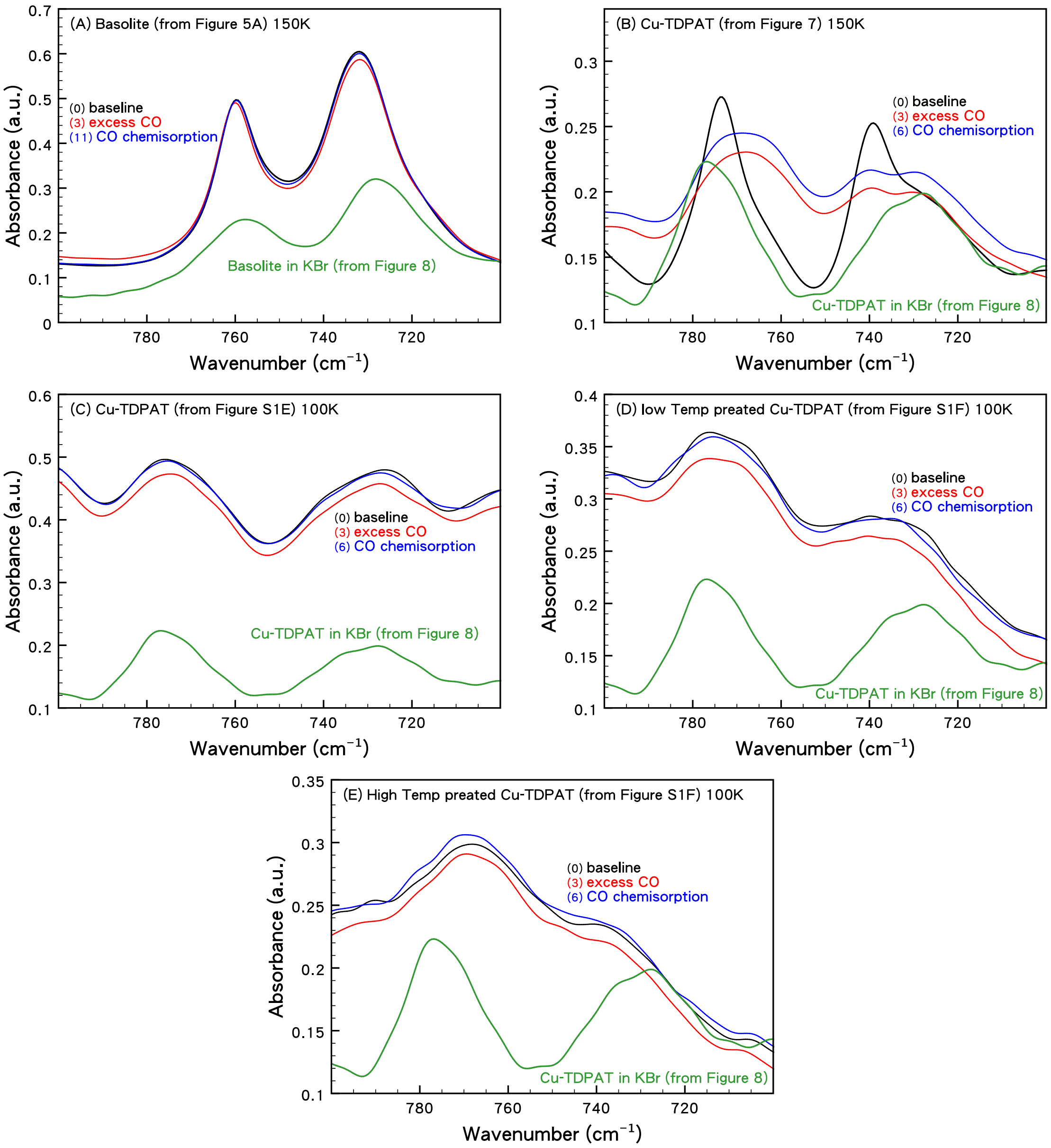

Figure S11: The FTIR fingerprint region (Cu-O bend at ~760 cm^{-1}) of (A) **B**(SA) at 150 K, (B) **T** at 150 K, (C) **T** at 100 K, (D) **T** at 100 K with low temperature pretreatment, and (E) **T** at 100 K with high temperature pretreatment. The green spectra is MOF in KBr as references at 300 K.

Except for **T** at 150 K with minor (4 cm^{-1}) shift, mainly no peak shift in Cu-O peak is observed before and after CO exposure.

Table S3: The stabilized FTIR spectra under 0.34 bar Ar purging curve fitting parameters of **B**(SA) and **B**(RU)-1 from Figure S3.

MOF	Figure S3	Peak Position (cm^{-1})	Intensity (a.u.)	FWHM (cm^{-1})	Gaussian-Lorentzian	Peak Area (%)
B(SA)	**A**	2123	0.15	38	0.57	48.9
		2169	0.34	9.0	0.00	43.7
		2156	0.032	17	1.00	4.4
		2190	0.010	20	0.00	3.0
	B	2172	0.032	12	0.34	12.4
		2120	0.086	36	1.00	87.6
B(RU)-1	**C**	2125	0.15	39	0.08	58.2
		2169	0.19	13	0.03	26.7
		2156	0.032	13	1.00	3.1
		2188	0.044	25	0.03	12.0
	D	2171	0.041	12	0.00	26.7
		2133	0.062	36	0.63	73.3

Reference

1 *Infrared spectroscopy correlation table*

2 *http://orgchem.colorado.edu/Spectroscopy/irtutor/aminesir.html*

3 *http://wwwchem.csustan.edu/Tutorials/INFRARED.HTM*

4 P.A. Redhead*Vacuum,* 1962, **12,** 203.